



Heriot-Watt University  
Research Gateway

# Surface heterogeneity and inhomogeneous broadening of vibrational line profiles

## Citation for published version:

Taj, S, Baird, D, Rosu-Finsen, A & McCoustra, MRS 2017, 'Surface heterogeneity and inhomogeneous broadening of vibrational line profiles', *Physical Chemistry Chemical Physics*, vol. 19, no. 11, pp. 7990-7995. <https://doi.org/10.1039/C6CP07530D>

## Digital Object Identifier (DOI):

[10.1039/C6CP07530D](https://doi.org/10.1039/C6CP07530D)

## Link:

[Link to publication record in Heriot-Watt Research Portal](#)

## Document Version:

Peer reviewed version

## Published In:

Physical Chemistry Chemical Physics

## Publisher Rights Statement:

© Royal Society of Chemistry 2017

## General rights

Copyright for the publications made accessible via Heriot-Watt Research Portal is retained by the author(s) and / or other copyright owners and it is a condition of accessing these publications that users recognise and abide by the legal requirements associated with these rights.

## Take down policy

Heriot-Watt University has made every reasonable effort to ensure that the content in Heriot-Watt Research Portal complies with UK legislation. If you believe that the public display of this file breaches copyright please contact [open.access@hw.ac.uk](mailto:open.access@hw.ac.uk) providing details, and we will remove access to the work immediately and investigate your claim.



## Surface Heterogeneity and Inhomogeneous Broadening of Vibrational Line Profiles

Journal:	<i>Physical Chemistry Chemical Physics</i>
Manuscript ID	CP-ART-11-2016-007530.R1
Article Type:	Paper
Date Submitted by the Author:	n/a
Complete List of Authors:	Taj, Skandar; Heriot-Watt University, Institute of Chemical Sciences Baird, Diane; Heriot-Watt University, Institute of Chemical Sciences Rosu-Finsen, Alexander; Heriot-Watt University, Institute of Chemical Sciences McCoustra, Martin; Heriot-Watt University, Institute of Chemical Sciences

Article type: Full paper

**PCCP**

Physical Chemistry Chemical Physics



Website [www.rsc.org/pccp](http://www.rsc.org/pccp)

Impact factor\* 4.449

**Journal expectations** To be suitable for publication in *Physical Chemistry Chemical Physics* (PCCP) articles must include significant new insight into physical chemistry.

**Article type: Full paper** Original scientific work that has not been published previously. Full papers do not have a page limit and should be appropriate in length for scientific content.

**Journal scope** Visit the [PCCP website](http://www.rsc.org/pccp) for additional details of the journal scope and expectations.

PCCP is an international journal for the publication of cutting-edge original work in physical chemistry, chemical physics and biophysical chemistry. To be suitable for publication in PCCP, articles must include significant new insight into physical chemistry; this is the most important criterion that reviewers should judge against when evaluating submissions. Example topics within the journal's broad scope include:

- Spectroscopy
- Dynamics
- Kinetics
- Statistical mechanics
- Thermodynamics
- Electrochemistry
- Catalysis
- Surface science
- Quantum mechanics
- Theoretical research

Interdisciplinary research areas such as polymers and soft matter, materials, nanoscience, surfaces/interfaces, and biophysical chemistry are also welcomed if they demonstrate significant new insight into physical chemistry.

**Reviewer responsibilities** Visit the [Reviewer responsibilities website](http://www.rsc.org/pccp) for additional details of the reviewing policy and procedure for Royal Society of Chemistry journals.

When preparing your report, please:

- Focus on the originality, importance, impact and reliability of the science. English language and grammatical errors do not need to be discussed in detail, except where it impedes scientific understanding.
- Use the [journal scope and expectations](http://www.rsc.org/pccp) to assess the manuscript's suitability for publication in PCCP.
- State clearly whether you think the article should be accepted or rejected and include details of how the science presented in the article corresponds to publication criteria.
- Inform the Editor if there is a conflict of interest, a significant part of the work you cannot review with confidence or if parts of the work have previously been published.

Thank you for evaluating this manuscript, your advice as a reviewer for PCCP is greatly appreciated.

**Dr Sam Keltie** Executive Editor  
Royal Society of Chemistry, UK

**Professor Seong Keun Kim** Editorial Board Chair  
Seoul National University, Korea



Journal Name

ARTICLE

## Surface Heterogeneity and Inhomogeneous Broadening of Vibrational Line Profiles

Skandar Taj, Diane Baird, Alexander Rosu-Finsen\* and Martin R. S. McCoustra

Received 00th January 20xx,  
Accepted 00th January 20xx

DOI: 10.1039/x0xx00000x

www.rsc.org/

The surface heterogeneity of amorphous silica (aSiO<sub>2</sub>) has been probed using coverage dependent temperature programmed desorption (TPD) of a simple probe molecule, carbon monoxide (CO). The resulting distribution of interaction energies is the foundation from which an environmentally broadened vibrational line profile synthesis has been undertaken. These simulations are compared with measured line profiles recorded at 0.1 cm<sup>-1</sup> resolution using reflection-absorption infrared spectroscopy (RAIRS). A comparison of such line profile synthesis for CO on amorphous silica and on porous amorphous solid water (p-ASW) is also reported and conclusions are drawn as to the vibrational relaxation and surface dynamics of the CO molecule on the two surfaces.

### Introduction

Vibrational spectroscopy is a powerful family of techniques for the characterisation of molecules in a wide range of environments.<sup>1</sup> The vibrational spectra of molecules in condensed phases are sensitive to the local environment in which the molecules find themselves. Both vibrational frequencies and line profiles reflect that sensitivity.

Vibrational frequencies shift reflecting changes in both force fields, because of intermolecular interaction induced changes in electron density distributions around vibrational chromophores, and mass distributions. Over the years, many empirical correlations have been established reflecting the impact of environment on vibrations for both chromophores in isolated molecules,<sup>2</sup> as exemplified by the carbonyl C=O chromophore,<sup>3</sup> and chromophores in molecular clusters, especially hydrogen-bonded systems.<sup>4</sup>

Fermi's Golden Rule and the energy-time Uncertainty Principle ultimately govern vibrational line profiles, like those of other spectroscopic transitions, and yield symmetric Lorentzian profiles for vibrational transitions in isolated molecules.<sup>5</sup> Efficient non-radiative mechanisms reduce vibrational excited state lifetimes and hence homogeneously, and symmetrically, broaden linewidths often resulting in Gaussian or Voigt line profiles. In the gas phase, temperature (average molecular speed – Doppler Broadening) and pressure (collision frequency – Pressure Broadening) are the principle broadening mechanisms resulting in homogeneous broadening of gas phase line profiles.<sup>6</sup> On solid surfaces, molecular translation and rotation are frustrated and weakly interacting adsorbates on simple ionic solids can therefore exhibit relatively narrow linewidths. The classic example of this is found in the work of Ewing and co-workers.<sup>7,8</sup> These authors estimate the natural linewidth for the vibration of carbon monoxide (CO) on the NaCl (100) surface at 5 K to be of the order of 10<sup>-8</sup> cm<sup>-1</sup>, and suggest that the observed linewidth, 0.07 cm<sup>-1</sup>, results from the residual

heterogeneity of the NaCl surface.<sup>7,8</sup> In contrast, on metal surfaces, vibrating dipoles couple with the free electrons in the metal band structure providing a fast and efficient mechanism for relaxing excited adsorbate vibrations *via* electron-hole pair creation.<sup>9,10</sup> The resulting line profiles are broad, for example varying from around 5 to 15 cm<sup>-1</sup> for CO on metal single crystal surfaces, and asymmetric, reflecting Fano coupling between the adsorbate vibration and the non-adiabatic electron-hole pair continuum of the substrate.<sup>11,12</sup> Additionally, these systems, as with halide surfaces, are often subject to further broadening due to environmental heterogeneity.<sup>13</sup> Environmental heterogeneity reaches its extreme with the profiles of vibrational lines of adsorbates interacting with supported metal and metal oxide catalysts.<sup>14</sup>

As illustrated by the few examples above, it is clear that CO is a very sensitive environmental probe. However, its utility as such extends far beyond Earth-bound laboratories with its widespread use in remotely probing both the gas phase and solid state in astrophysical environments.<sup>15-18</sup> This is nicely illustrated by a combination of observation<sup>16</sup> and experiment<sup>19</sup> that has tentatively identified CO directly bound to silicate surfaces in some cold, dense environments.

Recently, a combination of vibrational spectroscopy at cryogenic temperatures and computational investigations has permitted the derivation of a vibrational frequency – interaction energy correlation for CO in a variety of cluster and surface bound environments.<sup>20</sup> The linear X...CO interaction particularly shows a strong linear correlation,

$$\Delta\bar{\nu} / \text{cm}^{-1} = 3.330(E_b / \text{kJ mol}^{-1}) + 2.308 \quad (1)$$

between the vibrational wavenumber shift,  $\Delta\bar{\nu}$ , from the isolated CO vibrational wavenumber and the strength of the interaction experienced by the CO molecule in a particular environment,  $E_b$ . This nicely illustrates the sensitivity of the vibrational frequency of the CO molecule in the linear configuration to its interaction in complexes and on surfaces where the interactions are predominantly non-covalent in nature.

Thus, in systems demonstrating environmental heterogeneity where the strength of the interaction, or distribution of strengths, is

Address: Institute of Chemical Sciences, Heriot-Watt University, EDINBURGH, EH14 4AS, UK.

\*Author to whom correspondence should be directed: ar163@hw.ac.uk

known, the frequency shift(s) could be predicted and the CO vibrational line profile synthesised. This paper will demonstrate the feasibility of such environmentally broadened vibrational line profile synthesis from a knowledge of relevant environmental interaction energies for the case of CO on amorphous silica (aSiO<sub>2</sub>). The relevant interaction energies will be recovered from inversion of temperature programmed desorption (TPD) data as illustrated in reference [19]. In addition, in synthesising line profiles, this analysis should reveal something of the vibrational relaxation and surface dynamics of the CO molecule on aSiO<sub>2</sub> and so begin to explain the temperature invariant rather asymmetric line shape of the CO vibration reported in reference [19].

## Experimental

The experiments were conducted in an ultrahigh vacuum system described in detail previously.<sup>21,22</sup> Briefly, the central 30 cm diameter stainless steel chamber is pumped by a liquid nitrogen trapped diffusion pump (Edwards, EO6) backed by a mechanical rotary pump (Edwards, E2M18) to a base pressure of  $2 \times 10^{-10}$  mbar after baking. The oxygen-free high-conductivity (OFHC) copper sample block is coated with a 300 nm thick aSiO<sub>2</sub> film deposited by electron-beam evaporation of fused silica<sup>23</sup> is mounted onto the end of a closed-cycle helium cryostat (APD, CH-202). The silica substrate is heated by a cartridge heater (Heatwave Labs, Inc.) embedded in the OFHC copper substrate and surface temperatures are monitored using a KP (Gold-Chromel) thermocouple. The chamber is equipped with a line-of-sight quadrupole mass spectrometer (Hiden Analytical Ltd, HAL301) for TPD and FTIR spectrometer (Varian 670-IR) and associated optics for RAIRS.

CO (CK Special Gases Ltd., 99.997% purity) and H<sub>2</sub>O (Fluka, 99.9% purity) was deposited by background dosing onto the aSiO<sub>2</sub> substrate held at 18 K, at which all experiments were conducted. Exposures of the sample to the gas are expressed in monolayer (ML) estimated from the corresponding exposure assuming unit sticking probability. TPD is performed by applying a heating ramp of  $0.1 - 0.5 \text{ K s}^{-1}$  to a suitable final surface temperature. Desorbing species were detected using the quadrupole mass spectrometer (QMS). Consecutive TPD experiments, from 0.2 to 1 ML, were conducted on the same day. Build-up of gas-phase CO or degassing of CO from the chamber walls is considered negligible due to the limited overall daily dose of 3 ML. Further to this, the QMS monitored CO dosing ( $m/z = 12, 14$  and  $28$ ) to verify the purity of CO. A line-of-sight housing around the QMS ensured that the TPD data was collected only from the heated substrate. RAIR spectra were measured at a 75° angle incidence to the normal of the surface; the infrared radiation being collected by a MCT detector cooled with liquid nitrogen. Spectra were recorded at an instrument-limited resolution of  $0.1 \text{ cm}^{-1}$  by co-addition of 512 scans at the base temperature of the UHV system.

## Results and Discussion

### CO on Amorphous Silica

Figure 1 presents a RAIR spectrum of 0.6 ML CO on aSiO<sub>2</sub> at 18 K in the sub-monolayer regime. The line profile is clearly asymmetric with typical full-width-at-half-maximum (FWHM) of  $5.6 \text{ cm}^{-1}$ ; considerably larger than the  $0.1 \text{ cm}^{-1}$  instrument-limited resolution used in recording the spectra. As there is no fundamental reason for an asymmetric profile on an insulator surface such as aSiO<sub>2</sub>, the observed line profiles must be determined by a combination of

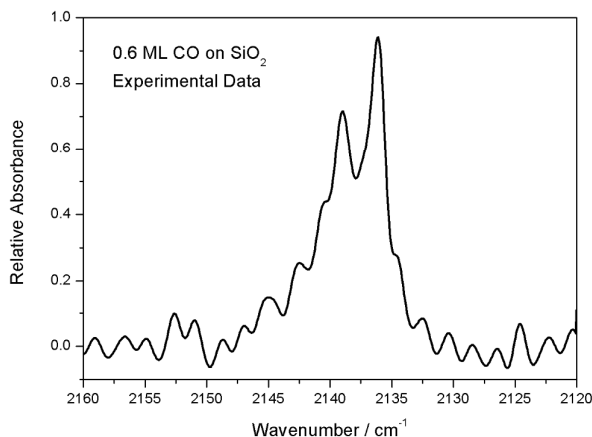


Figure 1: Baselined RAIR spectrum of 0.6 ML CO on aSiO<sub>2</sub>.

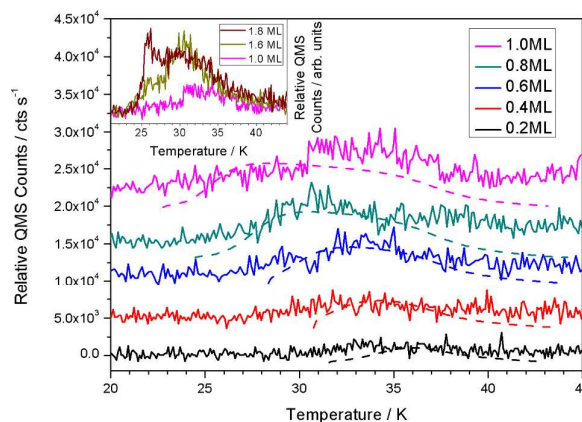
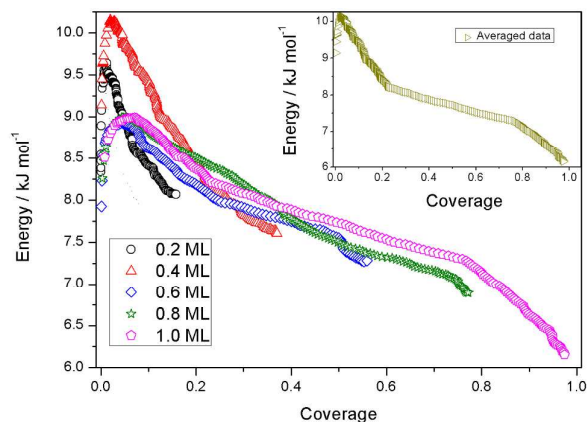


Figure 2: TPD data for sub-monolayer quantities of CO desorbing from aSiO<sub>2</sub> as a function of the indicated exposures in monolayers recorded on  $m/z = 12$   $m_u$ . The individual TPD traces have been offset for clarity with the dashed lines relating to TPD simulations. The insert contains the sub-monolayer to multilayer transition for CO on aSiO<sub>2</sub>.

environmental heterogeneity in addition to homogeneous broadening associated with relaxation of the excited CO vibration through its weak mechanical coupling with the vibrations of the aSiO<sub>2</sub> substrate.

The TPD data for CO desorbing from aSiO<sub>2</sub> are shown in Figure 2 and exhibit coincident trailing edges at low exposures and a common leading edge at higher exposures as shown in the insert. The dashed lines are the results of sub-monolayer  $E_{\text{des}}$  simulations based on a previously used FORTRAN 90 model<sup>24</sup>, the use and relevance of this model will be discussed later in this section. The data in the insert is consistent with multilayer growth as seen from the clear shift in the leading edge of desorption. This allows us to identify the exposure necessary to generate a monolayer coverage on the aSiO<sub>2</sub> surface, which is estimated to contain  $2.88 \times 10^{15} \text{ molecules cm}^{-2}$ . Hence, we can define CO surface coverages for all exposures. The coincidence in trailing edges is usually associated with recombinative second-order desorption, however there is no evidence to suggest that CO dissociates on aSiO<sub>2</sub> at low temperature. Rather, the aSiO<sub>2</sub> surface presents a range of binding sites with different binding energies for adsorption.<sup>25</sup> The trailing edge alignment indicates that the molecules are mobile enough on the aSiO<sub>2</sub> surface to find the deepest, energetically most favourable binding sites. Consequently, molecules situated in weaker binding



**Figure 3:**  $E_{\text{des}}$  as a function of  $N_{\text{ads}}$ , the surface concentration of adsorbed CO for background dosed sub-monolayers of CO with averaged data in the insert.

sites desorb first, resulting in desorption peak broadening. Since the assumption of a single value for the activation energy of desorption,  $E_{\text{des}}$ , is no longer valid, direct inversion of the Polanyi–Wigner Equation (2):

$$r_{\text{des}} = -\frac{dN_{\text{ads}}(t)}{dt} = \nu N_{\text{ads}}(t)^n e^{-E_{\text{des}}/k_B T} \quad (2)$$

where  $\nu$  is the pre-exponential factor,  $n$  and  $E_{\text{des}}$  the desorption order and energy,  $k_B$  the Boltzmann constant and  $T$  the surface temperature, can be used to derive  $E_{\text{des}}$  as function of the surface concentration at time  $t$ ,  $N_{\text{ads}}(t)$ :

$$E_{\text{des}}(N_{\text{ads}}(t)) = -k_B T \ln \left( \frac{dN_{\text{ads}}(t)}{dt} \frac{1}{\nu N_{\text{ads}}(t)^n} \right) \quad (3)$$

Tait *et al.*<sup>26</sup> first reported this method and it has been adapted since in studies of small molecule desorption from environmentally heterogeneous surfaces.<sup>19,25</sup>  $dN_{\text{ads}}(t)/dt$  is simply determined from the QMS count rate as in the high pumping speed regime of TPD,  $r_{\text{des}}$  is proportional to the measured change in partial pressure of the desorbing CO. Given that we are considering first order desorption in an adsorption system dominated by van der Waals interactions,  $n$  and  $\nu$  are 1 and  $1 \times 10^{12} \text{ s}^{-1}$ , respectively. The values of  $N_{\text{ads}}(t)$  were determined by subtracting the total gas phase concentration at the previous time step from the initial surface concentration,  $N_{\text{tot}}$ .  $N_{\text{tot}}$  is equal to the rate of bombardment,  $Z_w$ , multiplied by the dosing time,  $\tau$ , (4):

$$N_{\text{tot}} = Z_w \tau = \frac{PS\tau}{\sqrt{2\pi m k_B T}} \quad (4)$$

where  $P$  is the pressure (in Pascal),  $S$  the sticking coefficient and  $m$  the mass of a single CO molecule (in kg). At the low surface temperatures employed in this study, desorption is negligible and all molecules are assumed to stick to the surface. Hence,  $S$  is 1.

A summary of the experimental results can be seen in Table 1. The range of  $E_{\text{des}}$  values decrease with increasing coverage as expected and illustrated in the literature.<sup>19,27</sup> The uncertainty related to the desorption energy stems from the uncertainty in the temperature measurements ( $\pm 0.5 \text{ K}$ ). FWHM measurements of each coverage are shown as estimated from the baselined RAIR spectra where the uncertainty is due to the resolution of the FT-IR spectrometer ( $\pm 0.1 \text{ cm}^{-1}$ ). The linewidth is calculated from the

CO Coverage / ML	$E_{\text{des}} / \text{kJ mol}^{-1}$ ( $\pm 0.5$ )	FWHM / $\text{cm}^{-1}$ ( $\pm 0.1$ )	$\delta / \text{cm}^{-1}$ ( $\pm 0.05$ )
0.2	8.1 – 9.6	5.0	2.1
0.4	7.6 – 10.2	5.4	2.3
0.6	7.3 – 8.9	5.6	2.5
0.8	6.9 – 9.0	6.5	2.8
1.0	6.2 – 9.0	6.7	2.9

**Table 1:** This table shows the experimental values extracted from the TPD and RAIRS experiments of the various CO coverages.  $\delta$  are the linewidths of the vCO features.

FWHM as stated in Equation 8, however this will be discussed in further detail later in this work. Further to this, the integrated absorption scales linearly with each coverage in the sub-monolayer regime as might be expected from the Beer-Lambert law.

Plots of  $E_{\text{des}}$  against  $N_{\text{ads}}(t)$  are constructed for each sub-monolayer CO dose (Figure 3) from the experimental data presented in Figure 2 along with Equations 2, 3 and 4. A full analysis involving models of the experimental CO data have previously been detailed for the substrate used in this work<sup>19</sup> and other aSiO<sub>2</sub> surfaces.<sup>27</sup> The averaged data as seen in the insert in Figure 3 will be used from hereon as a representation of the distribution of interaction energies of CO molecules with the aSiO<sub>2</sub> surface. Our basis for saying this can be seen when returning to Figure 2. Here, the dashed lines are the results of sub-monolayer desorption simulations where the coverage dependant  $E_{\text{des}}$  from the insert in Figure 3 is used in the simulation of all our TPD measurements. As can be seen in Figure 2, the data and simulations are consistent and shift toward lower temperature as the coverage increases. This is as expected, when wetting molecules transition from sub-monolayer, to monolayer and on to multilayers. With this said, we use the averaged  $E_{\text{des}}$  distribution from Figure 3 to derive the likelihood of CO adsorption at a particular site with a given  $E_{\text{des}}$  i.e., the value of  $P(E_{\text{des}}) \cdot P(E_{\text{des}})$  is given by (5):

$$P(E_{\text{des}}) = -\frac{dN_{\text{ads}}}{dE_{\text{des}}} \quad (5)$$

Figure 4 shows  $P(E_{\text{des}})$  versus  $E_{\text{des}}$  for the CO-aSiO<sub>2</sub> system under consideration. The distribution recovered is not dissimilar to those reported for CO and other small molecules on a number of heterogeneous surfaces.<sup>19,25,26,278,29</sup> Clearly, Figure 4 defines the range of interaction energies associated with the surface heterogeneity on the aSiO<sub>2</sub> surface. However, it also gives us the

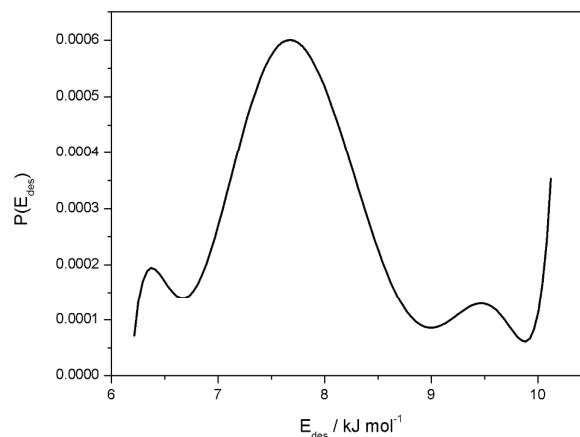


**Figure 4:**  $P(E_{\text{des}})$  versus  $E_{\text{des}}$  as derived from sub-monolayer TPD of CO from our aSiO<sub>2</sub> substrate.



weighting factor associated with each of those energies, *i.e.* the probability that a CO molecule landing randomly on the aSiO<sub>2</sub> surface will find itself in such an environment. Figure 4 is thus central to the simulation of the CO vibrational line profile in this heterogeneous environment.

The line profile synthesis itself is a relatively simple process as outlined in the sequence below;

- (1)  $E_b$  in equation (1) is equated with  $E_{des}$  and the wavenumber shifts,  $\Delta\bar{\nu}(E_{des})$ , calculated for the relevant range of  $E_{des}$ ;
- (2) The CO vibrational line positions,  $\bar{\nu}(E_{des})$ , are calculated at each  $E_{des}$  according to (6)

$$\bar{\nu}(E_{des}) = \bar{\nu}_0 + \Delta\bar{\nu}(E_{des}) \quad (6)$$

where  $\bar{\nu}_0$  is the vibrational origin and can be thought of as representing the vibrational wavenumber of CO on non-interacting aSiO<sub>2</sub> surface, *i.e.* it encompasses the effect of the mass of the silica surface on the CO vibration;

- (3) The vibrational line intensity at each line position,  $I(\bar{\nu}, E_{des})$ , is calculated assuming a simple Gaussian line profile (7) due to thermal broadening;

$$I(\bar{\nu}) = I_0 \sum_{E_{des}} P(E_{des}) e^{-[\bar{\nu} - \bar{\nu}(E_{des})]^2 / 2\delta^2} \quad (7)$$

where  $\delta$  controls the width of the Gaussian shape (sometimes referred to as the Gaussian RMS width) and is related to the FWHM according to (8)

$$FWHM = 2\sqrt{2 \ln(2)}\delta \quad (8)$$

and  $I_0$  is simply an intensity scaling factor. The overall line profile is obtained by summing over  $E_{des}$ .

- (4) The parameters,  $\bar{\nu}_0$ ,  $\delta$  and  $I_0$ , are varied until a good reproduction of the experimental line profile is obtained.

Figure 5 compares the simulated CO vibrational line profile on an aSiO<sub>2</sub> surface with that obtained experimentally. The best-fit parameters,  $\bar{\nu}_0$  and  $\delta$ , are listed in Table 2. Figure 5A shows the effect of the full distribution of interaction energies recovered from

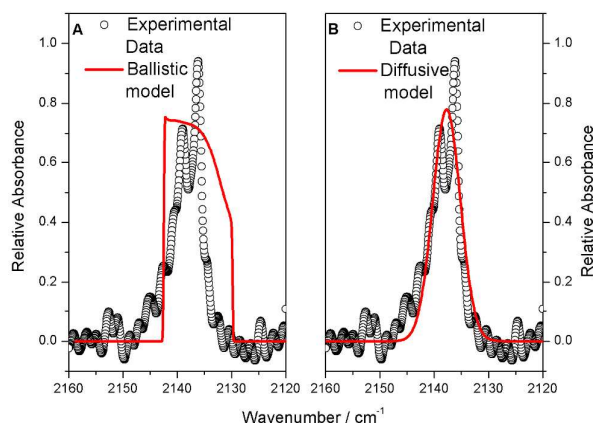


**Figure 5:** Comparison of the experimental (open circles) and modelled (red line) data of CO on aSiO<sub>2</sub>. The experimental data is of 0.6 ML CO at 18 K and exhibits a FWHM of 5.6 cm<sup>-1</sup>. (A) shows the simulated line profile when CO is ballistically deposited with a FWHM of 12.5 cm<sup>-1</sup>. (B) shows how a better fit is obtained when CO is free to diffuse using the inverse Boltzmann weighted distribution of  $E_{des}$  and leads to a best-fit FWHM of 5.9 cm<sup>-1</sup>. A point to note is the sub-structure in the experimental line profiles which is due to overlapping features from gas-phase water in the optics purge gas outside of the UHV chamber.

the TPD inversion. This would represent the situation where the CO is ballistically deposited, *i.e.* random deposition without subsequent diffusion on the surface ("stick and stop" as it is sometimes referred to). **The model shown in Figure 5A is the best fit given the ballistic deposition conditions and does not fit the data well. The model is made from the full  $E_{des}$  distribution from Figure 4 and a simulated linewidth of 2.5 cm<sup>-1</sup> (compared to the experimental resolution of 0.1 cm<sup>-1</sup>) which yields a FWHM of 12.5 cm<sup>-1</sup>.** On the other hand, Figure 5B illustrates the effect of restricting the accessible energies to only the strongest interactions, *i.e.* permitting diffusion of the CO over the aSiO<sub>2</sub> surface even at 18 K. This is achieved by introducing an inverse Boltzmann weighting to (7),

$$I(\bar{\nu}) = I_0 \sum_{E_{des}} P(E_{des}) e^{-E_{des}/RT} e^{-[\bar{\nu} - \bar{\nu}(E_{des})]^2 / 2\delta^2} \quad (9)$$

such that the strongest interactions are favoured. This latter situation provides a much better reproduction of the experimental data and is consistent with reference [19].

The best-fit FWHM for the vibrational line profile of CO on aSiO<sub>2</sub> is 5.9 cm<sup>-1</sup>, which should be compared with the measured FWHM of 5.6 cm<sup>-1</sup>. The difference between these quantities and the asymmetry of the line profile clearly arise from the heterogeneity of the aSiO<sub>2</sub> surface. The best-fit value, moreover, points to relatively slow vibrational energy redistribution from the CO vibration into the aSiO<sub>2</sub> phonon bath. This should be contrasted to the situation for CO on porous amorphous solid water (p-ASW); the subject of the next section.

#### CO on Porous Amorphous Solid Water

To illustrate the generality of the procedure described above, simulations of the vibrational lines profile for CO on p-ASW were undertaken. In approaching this problem, we have utilised the  $P(E_{des})$  versus  $E_{des}$  data of Kay and co-workers.<sup>29</sup> Figure 6 shows the comparison of the experimental and simulated line shapes. It should be noted that the vibrational spectrum of sub-monolayer coverages of CO adsorbed on p-ASW at 20 K exhibits two strong features at 2139 and 2153 cm<sup>-1</sup>, respectively.<sup>30,31</sup> The 2153 cm<sup>-1</sup> peak disappearing as the H<sub>2</sub>O film is annealed and pore collapse takes place in the p-ASW such that at temperatures above 80 K only

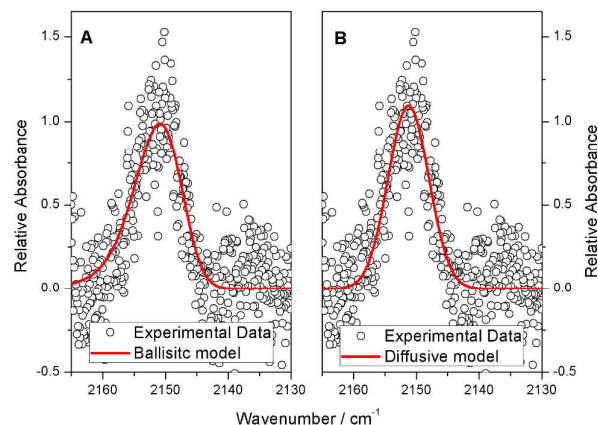


**Figure 6:** Comparison of the experimental CO stretching band, recorded with the instrument limited resolution, for 5 ML of CO on a p-ASW on our aSiO<sub>2</sub> substrate at base temperature (18 K) in UHV with a simulation derived from the data in [20, 29]. (A) shows the simulated ballistic line profile for a linewidth of 2.6 cm<sup>-1</sup> where the experimental data is collected at the instrument limit of 0.1 cm<sup>-1</sup> and (B) is a best-fit diffusive linewidth of 3.2 cm<sup>-1</sup>.

	$\bar{\nu}_0 / \text{cm}^{-1}$ ( $\pm 0.5$ )	$\delta / \text{cm}^{-1}$ ( $\pm 0.2$ )	Model FWHM / $\text{cm}^{-1} (\pm 0.5)$	Exp. FWHM / $\text{cm}^{-1} (\pm 0.1)$
CO on aSiO <sub>2</sub>	2075.5	2.5	5.9	5.6
CO on p-ASW (Ballistic)	2108.0	2.6	9.0	8.0
CO on p-ASW (Diffusive)	2089.0	3.2	7.6	8.0

**Table 2:** Comparison of the best-fit parameters,  $\bar{\nu}_0$  and  $\delta$ , and of the corresponding FWHM for the modelled and experimental CO vibrational line profiles on aSiO<sub>2</sub> and p-ASW.

the 2139 cm<sup>-1</sup> band is observed. This leads to the conclusion that the 2153 cm<sup>-1</sup> feature can be associated with the extended geometry in reference 31, i.e. CO adsorbed in a linear configuration with a dangling OH group. While the 2139 cm<sup>-1</sup> band is attributed to the compact geometry, i.e. CO lying parallel to an OH group and perhaps interacting with more than one OH group. The contribution of this latter feature has been subtracted from the data presented in Figure 6 to allow clearer comparison with the environmental heterogeneity simulations of the profile. The best-fit parameters,  $\bar{\nu}_0$  and  $\delta$ , derived from the simulation are listed in Table 2.

Figure 6 shows the ballistic deposition and diffusive models as compared to the experimental data. This could indicate that CO is free to both hit-and-stick and diffuse at the same time. Comparing  $E_{\text{des}}$  values for CO on aSiO<sub>2</sub> (6 – 12 kJ mol<sup>-1</sup>) and CO on p-ASW (11 – 16 kJ mol<sup>-1</sup>)<sup>29</sup> indicates that CO is more strongly bound to the water surface. A widely accepted rule of thumb says that the barrier to surface diffusion is of the order of 10 – 15% of the system's  $E_{\text{des}}$ <sup>32</sup>. This leads to CO being freer to diffuse on aSiO<sub>2</sub> as compared to p-ASW, which can also be understood from Figure 5 and 6. Recent work<sup>33-35</sup> suggests that CO is relatively free to diffuse while about 10% CO molecules on p-ASW can be trapped in pores. This is also seen in Figure 6 as both a ballistic deposition model and a diffusive model fit the experimental data. From the experiments and data presented in this work, an amount of CO trapped or mobile cannot be estimated. However, while developing our thoughts from references [33 – 35] we suggest a diffusive model represents the experimental data to a better degree considering the FWHM as shown in Table 2.

The rather broader FWHM reported in Table 2 is also consistent with a more efficient vibrational relaxation mechanism. It is well known that there is a significant density of vibrational states in p-ASW around 2000 to 2400 cm<sup>-1</sup> associated with bulk ASW.<sup>36,37</sup> Interaction of the vibrational excited CO via a dangling OH bond would therefore provide a very direct route into a phonon bath that is absent in the case of aSiO<sub>2</sub>.

## Conclusions

In concluding this work, it is clear that a relatively simple, and generalizable, procedure can be used to synthesise the vibrational line profiles of CO in an environmentally heterogeneous surface adsorption system where the interactions between the CO and the substrate are dominated by weak, non-covalent interactions. The key requirement for such a synthesis is knowledge of the range of interaction energies and their weighting as encompassed by the  $P(E_{\text{des}})$  versus  $E_{\text{des}}$  utilised in this simulations. While these data were derived experimentally in the present work, there is no reason, in

principle, why similar distributions derived from high quality computational chemistry could not be used. The challenge in that situation would be in identifying both the size of the system to computational model that would accurately reproduce the  $P(E_{\text{des}})$  versus  $E_{\text{des}}$  data and the most cost-effective computational method to apply to that system.

In simulating these line profiles, we have also highlighted key differences in the vibrational relaxation (p-ASW is more effective than aSiO<sub>2</sub>) and surface dynamics (CO is to a certain extent locked in place on p-ASW but free to diffuse on aSiO<sub>2</sub> at 18 K) in these systems that contribute to our growing knowledge of the behaviour of CO on insulator surfaces.

Could this idea be itself inverted to derive  $P(E_{\text{des}})$  versus  $E_{\text{des}}$  information in systems? That is a challenging question. Logically with sufficient quality in the IR data, it might be possible to assume a functional form for  $P(E_{\text{des}})$  versus  $E_{\text{des}}$  and iteratively fit synthesised vibrational line profiles to observations using standard least squares minimisation tools. Whether the results of such a fit are robust remains the issue.

## Acknowledgements

The authors thank B. D. Kay and R. S. Smith for access to their  $P(E_{\text{des}})$  versus  $E_{\text{des}}$  data for CO on porous amorphous solid water. The authors acknowledge the support of the UK Science and Technology Facilities Council (STFC, ST/M001075/1), the UK Engineering and Physical Science Research Council (EPSRC, EP/D506158/1) and the European Community FP7-ITN Marie-Curie Programme (LASSIE project, grant agreement #238258). TS thanks STFC for a project studentship. ARF thanks HWU for a James Watt Scholarship.

## Notes and references

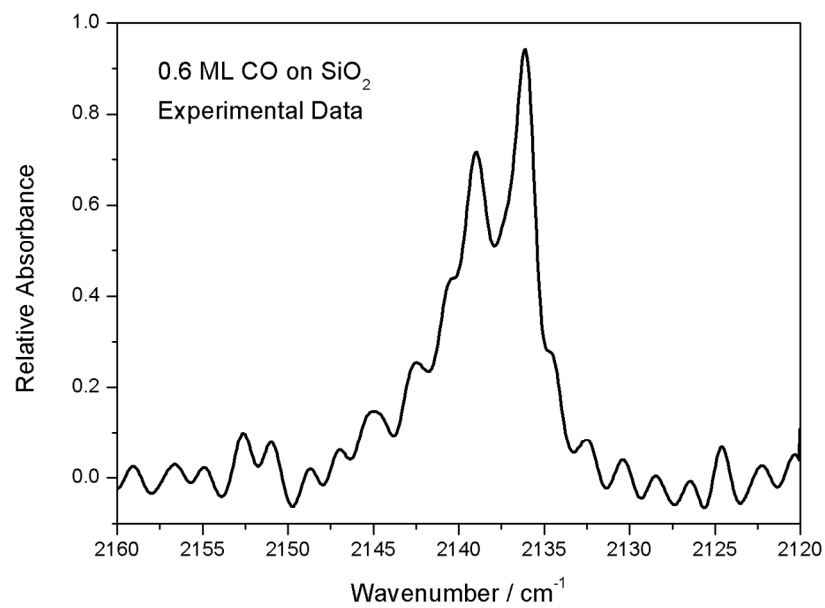
- J. M. Chalmers and P. R. Griffiths (eds), *Handbook of Vibrational Spectroscopy*, (Wiley, Chichester, 2001).
- R. M. Badger and S. H. Bauer, *J. Chem. Phys.*, 1937, **5**, 839.
- G. Horvath, J. Illenyi, L. Pusztay and K. Simon, *Acta Chim. Hung.*, 1987, **124**, 819.
- G. C. Pimentel and C. H. Sederholm, *J. Chem. Phys.*, 1956, **24**, 639.
- P. Atkins and R. Friedman, *Molecular Quantum Mechanics, Fourth Edition*, (Oxford University Press, Oxford, 2005) Chapter 6.
- W. Demtröder, *Laser Spectroscopy*, (Springer-Verlag, Heidelberg, 1982) Chapter 3.
- H. -C. Chang, C. Noda and G. E. Ewing, *J. Vac. Sci. Technol. A*, 1990, **8**, 2644.
- H. -C. Chang, D. J. Dai and G. E. Ewing, *J. Chin. Chem. Soc.*, 1995, **42**, 317.
- H. Ueba, *Prog. Surf. Sci.*, 1997, **55**, 115.
- H. Arnold, *Prog. Surf. Sci.*, 2011, **86**, 1.
- J.W. Gadzuk and A.C. Luntz, *Surf. Sci.*, 1984, **144**, 429.
- D.C. Langreth, *Phys. Rev. Lett.*, 1985, **54**, 126.
- R. Ryberg, *Phys. Rev. B*, 1985, **32**, 2671.
- J. Ryczkowski, *Catalysis Today*, 2001, **68**, 263.
- J. E. Chiar, P. A. Gerakines, D. C. B. Whittet, Y. J. Pendleton, A. G. G. M. Tielens, A. J. Adamson and A. C. A. Boogert, *Astrophys. J.*, 1998, **498**, 716.
- K. M. Pontoppidan, H. J. Fraser, E. Dartois, W. -F. Thi, E. F. van Dishoeck, A. C. A. Boogert, L. d'Hendecourt, A. G. G. M. Tielens and S. E. Bisschop, *S. E., Astron. Astrophys.*, 2003, **408**, 981.
- H. S. Liszt, *Astron. Astrophys.*, 2007, **476**, 291.
- W. -F. Thi, E. F. van Dishoeck, K. M. Pontoppidan and E. Dartois, *Mon. Not. Roy. Astron. Soc.*, 2010, **406**, 1409.



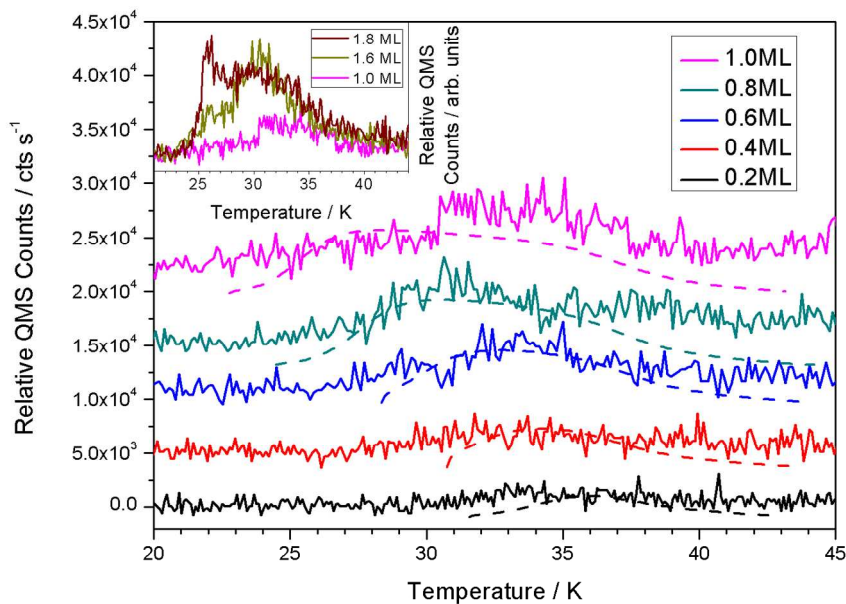
## ARTICLE

## Journal Name

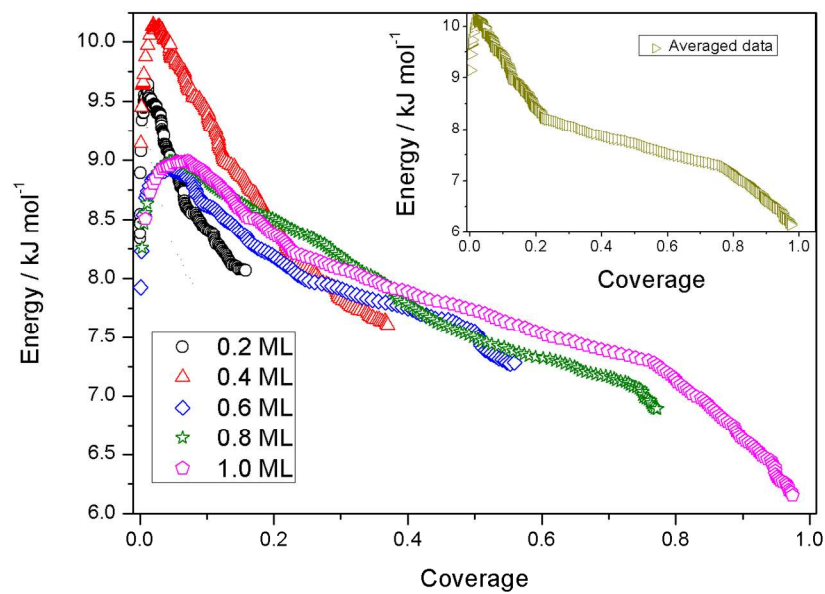
- 19 M.P. Collings, V.L. Frankland, J. Lasne, D. Marchione, A. Rosu-Finsen and M.R.S. McCoustra, *Mon. Not. Roy. Astron. Soc.*, 2015, **449**, 1826.
- 20 M. P. Collings, J. W. Dever and M. R. S. McCoustra, *Phys. Chem. Chem. Phys.*, 2014, **16**, 3479.
- 21 H. J. Fraser, M. P. Collings and M. R. S. McCoustra, *Rev. Sci. Instrum.*, 2002, **73**, 2161.
- 22 V. L. Frankland, A. Rosu-Finsen, J. Lasne, M. P. Collings and M.R.S. McCoustra, *Rev. Sci. Instrum.*, 2015, **86**, 055103.
- 23 J. D. Thrower, M. P. Collings, F. J. M. Rutten and McCoustra M.R.S., *Mon. Not. Roy. Astron. Soc.*, 2009, **394**, 1510.
- 24 J. D. Thrower, Ph.D. Thesis, 2009, Heriot-Watt University.
- 25 J. D. Thrower, M. P. Collings, F. J. M. Rutten and M. R. S. McCoustra, *J. Chem. Phys.*, 2009, **131**, 244711.
- 26 S. L. Tait, Z. Dohnalek, C. T. Campbell and B. D. Kay, *J. Chem. Phys.*, 2005, **122**, 164707.
- 27 J. A. Noble, E. Congiu, F. Dulieu and H. J. Fraser, *Mon. Not. R. Astron. Soc.*, 2012, **421**, 768.
- 28 J. A. Noble, S. Diana and F. Dulieu, *Mon. Not. Roy. Astron. Soc.*, 2015, **454**, 2636.
- 29 R. S. Smith, R. A. May and B. D. Kay, *J. Phys. Chem. B*, 2016, **120**, 1979.
- 30 M. P. Collings, J. W. Dever, H. J. Fraser, M. R. S. McCoustra and D. A. Williams, *Astrophys. J.*, 2003, **583**, 1058.
- 31 M. P. Collings, J. W. Dever, H. J. Fraser and M. R. S. McCoustra, *Astrophys. Space Sci.*, 2003, **285**, 633.
- 32 J.K. Nørskov, F. Studt, F. Abild-Pedersen and Thomas Bligaard, *Fundamental Concepts in Heterogenous Catalysis* (Wiley, Hoboken, 2014), p. 14.
- 33 F. Mispelaer, P. Theulé, H. Aouididi, J. Noble, F. Duvernay, G. Danger, P. Roubin, O. Morata, T. Hasegawa, and T. Chiavassa, *Astron. Astrophys.*, 2013, **555**, A13.
- 34 L. J. Karssemeijer, S. Ioppolo, M. C. van Hemert, A. van der Avoird, M. A. Allodi, G. A. Blake, and H. M. Cuppen, *Astrophys. J.*, 2014, **781**, 16.
- 35 T. Lauck, L. Karssemeijer, K. Shulenberger, M. Rajappan, K. I. Oberg, and H. M. Cuppen, *Astrophys. J.*, 2015, **801**, 118.
- 36 W. Hagen, A. G. G. M. Tielens and J. M. Tielens, *Chem. Phys.*, 1981, **56**, 367
- 37 J. P. Devlin, J. Sadlej and V. Buch, *J. Phys. Chem.*, 2001, **105**, 974



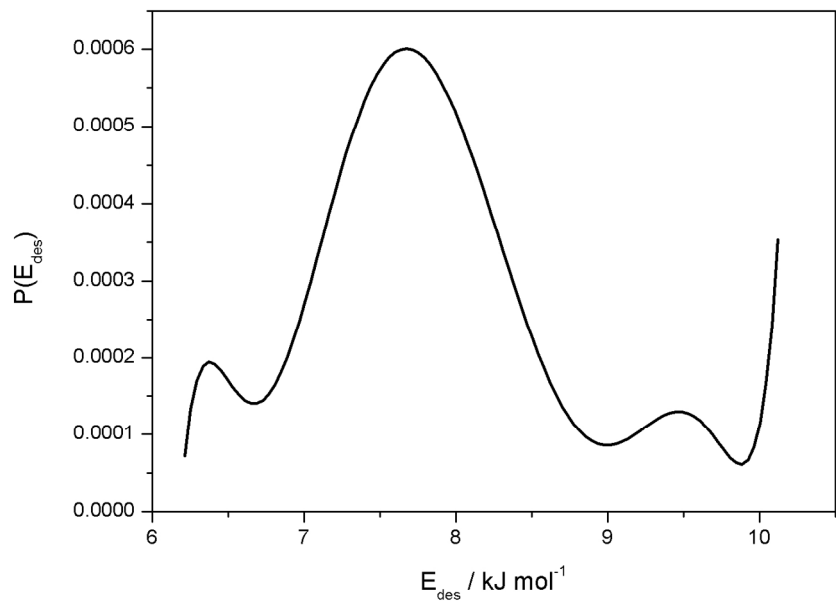
Baselined RAIR spectrum of 0.6 ML CO on aSiO<sub>2</sub>.



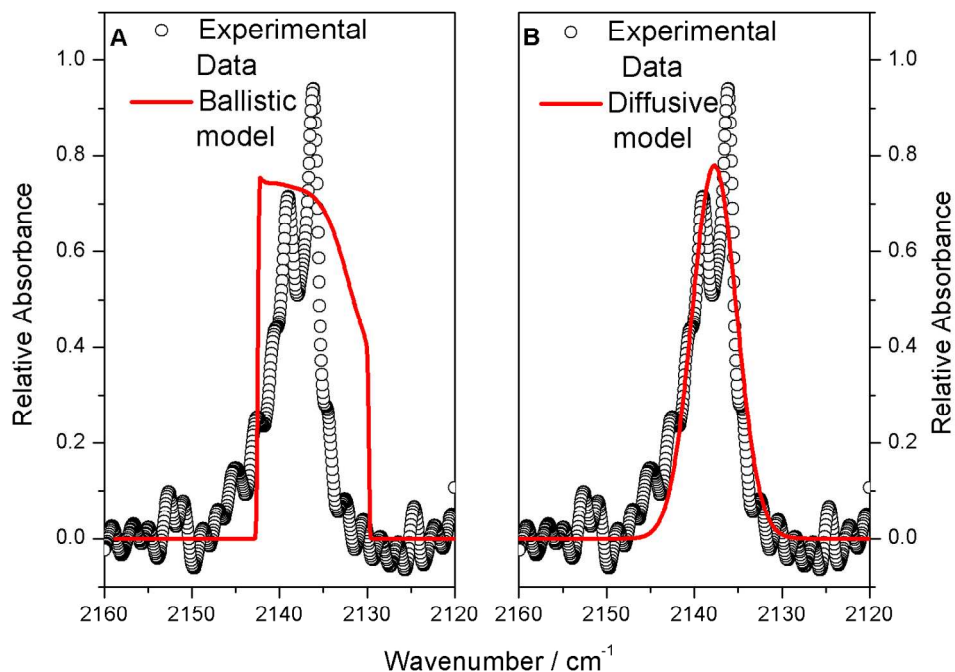
TPD data for sub-monolayer quantities of CO desorbing from aSiO<sub>2</sub> as a function of the indicated exposures in monolayers recorded on  $m/z = 12\ m_u$ . The individual TPD traces have been offset for clarity with the dashed lines relating to TPD simulations. The insert contains the sub-monolayer to multilayer transition for CO on aSiO<sub>2</sub>.



$E_{\text{des}}$  as a function of  $N_{\text{ads}}$ , the surface concentration of adsorbed CO for background dosed sub-monolayers of CO with averaged data in the insert.

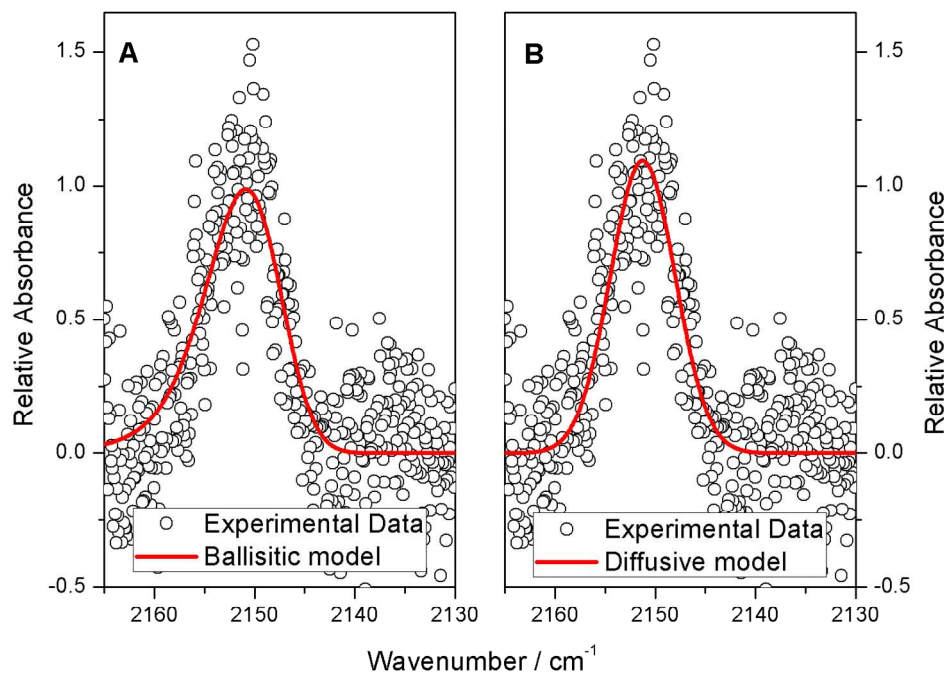


$P(E_{\text{des}})$  versus  $E_{\text{des}}$  as derived from sub-monolayer TPD of CO from our aSiO<sub>2</sub> substrate.



Comparison of the experimental (open circles) and modelled (red line) data of CO on aSiO<sub>2</sub>. The experimental data is of 0.6 ML CO at 18 K and exhibits a FWHM of 5.6 cm<sup>-1</sup>. (A) shows the simulated line profile when CO is ballistically deposited with a FWHM of 12.5 cm<sup>-1</sup>. (B) shows how a better fit is obtained when CO is free to diffuse using the inverse Boltzmann weighted distribution of  $E_{des}$  and leads to a best-fit FWHM of 5.9 cm<sup>-1</sup>. A point to note is the sub-structure in the experimental line profiles which is due to overlapping features from gas-phase water in the optics purge gas outside of the UHV chamber.





Comparison of the experimental CO stretching band, recorded with the instrument limited resolution, for 5 ML of CO on a p-ASW on our aSiO<sub>2</sub> substrate at base temperature (18 K) in UHV with a simulation derived from the data in [20, 29]. (A) shows the simulated ballistic line profile for a linewidth of 2.6 cm<sup>-1</sup> where the experimental data is collected at the instrument limit of 0.1 cm<sup>-1</sup> and (B) is a best-fit diffusive linewidth of 3.2 cm<sup>-1</sup>.

Reviewer comments are in RED and Author responses are in BLACK

**Referee: 1**

The manuscript shows an interesting approach to the topics of surface heterogeneity and offers a new tool to understand energy dissipation into the surface. Both of these topics are of interest to the physical chemical community as well as to astrochemists.

I do, however, recommend to expand the paper in terms of analysis and explanation and would recommend the authors to - if possible - perform some additional experiments. This will increase the quality of the paper and elevate it from a proof-of-principle level study. The conclusions drawn are clear and valid, but the story would benefit from additional insight.

We would like to thank the reviewer for taking the time to read through and comment on our work.

We also consider the work interesting for the physical sciences community and thank the referee for highlighting this potential impact of our work. The referee is correct that this is currently a proof-of-principle demonstration of a simple idea and while we are pursuing additional work it will take many months for the relevant computational and experimental work. This is easy to see from the extensive (many months) of work that went into the background paper on CO on molecular solid surfaces (Collings *et al.* *PCCP*, 2014, **16**, 3479). An equivalent study would have to be done for any new target molecule (*e.g.* CH<sub>4</sub> as suggested) along with the same type of TPD and RAIRS experiments as presented in the current paper. It would only be at this stage that the current analysis would become important. Having said this, we will state that we are currently extending our CO work to the CH<sub>3</sub>OH ice surface where there is little or no hydrogen bonding as solid methanol does not present dangling OH bonds at its surface. We also plan to move in the direction suggested by the referee of studying CH<sub>4</sub> in this manner.

Introduction

The authors state that energy dissipation on a metal surface is fast and efficient. In this light, can they comment on the fact that their a-SiO<sub>2</sub> substrate is coated on top of a Cu sample block? For instance, how thick is the a-SiO<sub>2</sub> layer?

The aSiO<sub>2</sub> layer is some 200 to 300 nm thick and is sufficiently thick to decouple the vibrating CO oscillator from the underlying free electron band structure of the Cu. CO adsorbs directly on Cu via a chemisorption interaction at about 100 K giving a typical CO vibrational frequency of 2086 cm<sup>-1</sup> and resonance width of 4 cm<sup>-1</sup>. The width of this transition reflects very rapid relaxation of the CO vibration due to electron-hole pair creation in the Cu. In addition, formally forbidden, due the metal surface selection rule, anti-absorption bands are observed at low frequency (around 400 cm<sup>-1</sup>) due to the presence of these electron-hole pairs which modify the surface resistivity of the Cu. Interposing the thick aSiO<sub>2</sub> spacer layer between the Cu and CO decouples the CO vibration from the metal electrons removing the rapid electron-hole pair relaxation channel and leaving only the mechanical coupling of the CO oscillator to the aSiO<sub>2</sub> lattice. We can qualitatively confirm this by recognising that the oscillator-metal interaction is essentially a dipole-image dipole interaction. Assuming, unrealistically that the image dipole will remain the same magnitude

moving the CO from around 2 nm when bound to the metal to around 200 nm or more when physisorbed on the aSiO<sub>2</sub>, the interaction will be reduced significantly. Such dipole-induced dipole interactions in the gas phase scale with  $z^6$  where  $z$  is the separation of the dipole centres of mass. Even if this is reduced to  $z^2$  or  $z^3$  on the surface due to restricted rotation, we are still taking about at least a  $10^4$  to  $10^6$  fold reduction in the strength of the interaction. The CO on the aSiO<sub>2</sub> therefore does not feel the effect of the metal and the vibrational dynamics will reflect that of the CO on aSiO<sub>2</sub> alone.

The following sentence in the experimental section has been modified to include the thickness of the aSiO<sub>2</sub> layer as written in **BOLD** words:

“The oxygen-free high-conductivity (OFHC) copper sample block is coated with **a 300 nm thick aSiO<sub>2</sub> film** deposited by electron-beam evaporation of fused silica<sup>23</sup> and is mounted onto the end of a closed-cycle helium cryostat (APD, CH-202)”.

### Experimental Section

Please state clearly in the Experimental section that the temperature of all experiments is 18 K.

This has been done by modifying this sentence to include the **BOLD** words:

“CO (CK Special Gases Ltd., 99.997% purity) and H<sub>2</sub>O (Fluka, 99.9% purity) was deposited by background dosing onto the aSiO<sub>2</sub> substrate held at 18 K, **at which all experiments were conducted.**”

Please state how many TPD's have been performed during a single experiment, i.e., per day. If more than one TPD has been done per day, please comment on the effect of CO sticking to the wall of the chamber, increasing the QMS baseline during the follow-up experiments.

The TPD experiments, ranging from 0.2 to 1.0 ML were done during the same day. Duplicate experiments, meant for verification of results were done on a different day.

While CO build-up can be a problem, we have disregarded it and not mentioned it here for a number of reasons:

- 1) The daily clean meant annealing the sample to about 220 K desorbing CO from the sample and cold finger. While at this temperature a titanium sublimation pump was fired for 3 minutes trapping oxygen containing species such as H<sub>2</sub>O and CO, while the diffusion pumps were doing their job.
- 2) With a cold sample (about 2 hours after annealing) and the FT-IR aligned, multiple background scans were collected with no changes monitored meaning adsorption of molecules such as CO was negligible.
- 3) The total amount of CO during the day reached a maximum of 3.0 ML
- 4) The QMS was on during CO dosing and the actual TPD experiments was initiated when the background CO count was at a plateau.

With this said, we have added these **BOLD** sentences in the experimental section for clarification:

“TPD is performed by applying a heating ramp of  $0.1 - 0.5 \text{ K s}^{-1}$  to a suitable final surface temperature. Desorbing species were detected using the quadrupole mass spectrometer (QMS). **Consecutive TPD experiments, from 0.2 to 1 ML, were conducted on the same day. Build-up of gas-phase CO or de-gassing of CO from the chamber walls is considered negligible due to the limited overall daily dose of 3 ML. Further to this, the QMS monitored CO dosing ( $m/z = 12, 14$  and  $28$ ) to verify the purity of CO. A line-of-sight housing around the QMS ensured that the TPD data was collected only from the heated substrate.** RAIR spectra were measured at a  $75^\circ$  angle incidence to the normal of the surface; the infrared radiation being collected by a MCT detector cooled with liquid nitrogen.”

Since QMS data are used and  $\text{N}_2$  has the same mass as CO, why have the authors not chosen to use  $^{13}\text{CO}$  for their experiments?

We did not have access to isotopically labelled CO, however during dosing and TPD experiments the QMS measured a variety of masses such as 12, 14 and 28 amu. However, the addition in the previous comment addresses this issue.

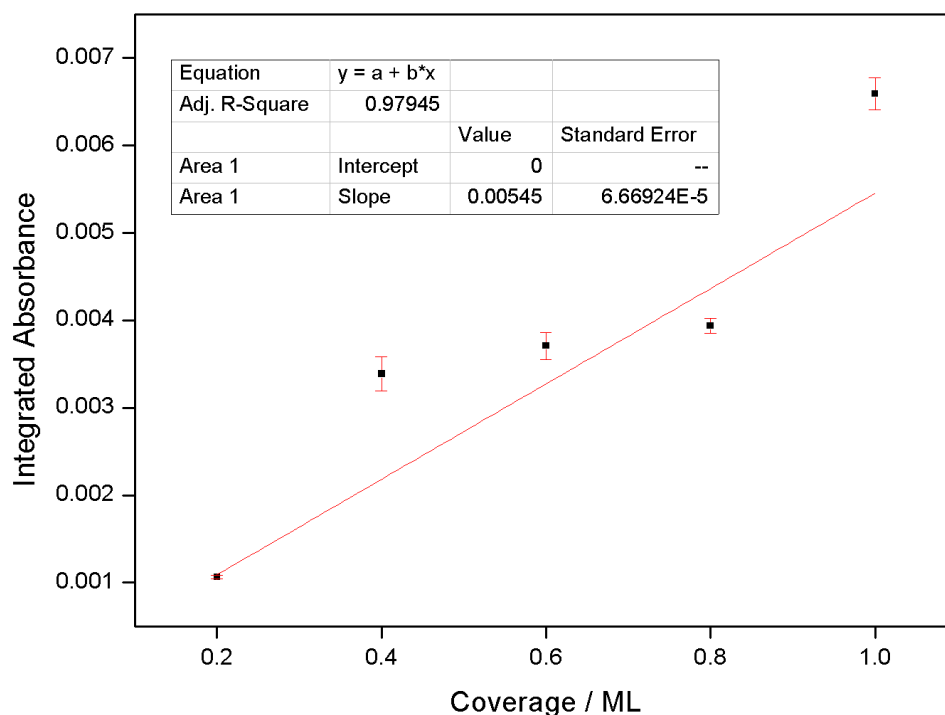
Why have experiments been performed only at 18 K? Do the authors expect that the ballistic model may be a better description if the experiment would be performed at a lower temperature?

Experiments were conducted at 18 K as this was the lowest temperature possible with this UHV rig. Besides comparing TPD data to IR data we have indicated that CO is able to diffuse at these low temperatures, in accordance to literature.

Conducting the same experiments at lower temperatures and comparing the data to the model would indeed be interesting. However, obtaining an even lower surface temperature would require a substantial investment in a new cryostat.

Can the authors correlate the one-monolayer coverage determined by TPD (Page 2, Results section) to infrared band strengths? This allows for an additional independent method of quantification.

This is an interesting question, and we thank the reviewer for raising it. Considering how CO wets the  $\text{aSiO}_2$  surface and forms a monolayer, such a correlation is possible. We have produced this graph from the experimental data:



This figure shows a linear IR absorbance increase with coverage as expected from adherence to the Beer-Lambert Law. However, the referee's questions highlights that we should not take this as read. In many studies of CO adsorption on metals, the Beer-Lambert Law is found to hold only at very low coverage where the adsorbate molecules are sufficiently far apart to be independent. When the coverage is increased and the adsorbates are close enough to interact through non-covalent interactions and dipole-dipole coupling, deviations from the Beer-Lambert Law are distinctly possible. The best known example of this is CO on the Pt(111) surface. Under those circumstances, one cannot rely on integrated intensities linearly depending on the surface concentration. However, TPD is not subject to this complication and gives a much more direct assessment of coverage. Thus explaining our choice of method for characterising the CO coverage on our surface.

To clarify the linear relationship between coverage and absorption, we have added the following to an already new addition. The sentence in bold relate to the Beer-Lambert Law:

**"... Further to this, the integrated absorption scales linearly with each coverage in the sub-monolayer regime as might be expected from the Beer-Lambert law.**

Plots of  $E_{\text{des}}$  against  $N_{\text{ads}}(t)$  are constructed for each sub-monolayer CO dose (Figure 3)..."

### Results & Discussion

Throughout the document there is no mentioning of any error bars, uncertainty analysis or S/N ratios. For instance Figs. 1 and 2 both seem to suffer from a poor S/N ratio. This may also strongly affect what is defined as 1.0 ML, since this is experimentally determined as I understood.

The monolayer is indeed experimentally determined from our TPD, which are recorded with the QMS in a line-of-sight shroud as in the work of Jones (S. G. Hessey and R. G. Jones, *Surf. Interface Anal.*, 2015, **47**, 587). It is well known that in true line-of-sight TPD there is

significant degradation of the S/N compared to simply placing the QMS face on to the sample. This is aggravated in our case due to the small amount of CO present from the need to be in the sub-monolayer regime. However, the advantages that accrue in further detailed analysis of the TPD outweigh the S/N issues.

To clarify the monolayer transitioning into a multilayer, we have added the data for 1.6 and 1.8 ML. These extra data sets show a common leading edge during desorption as is indicative of multilayer desorption.

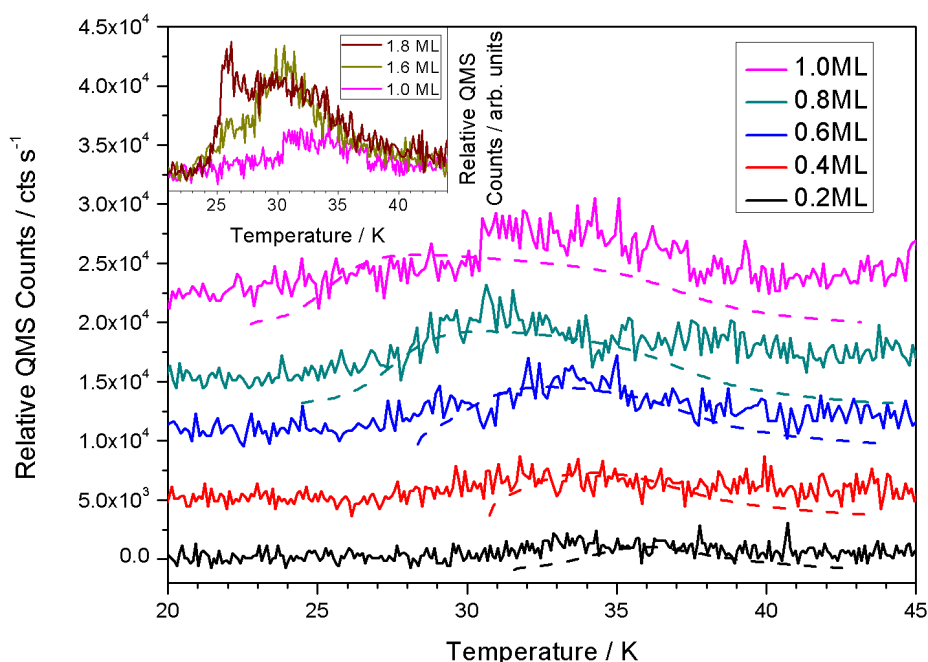
As to the S/N of our RAIRS measurements, these measurements were done at an instrument resolution of  $0.1\text{ cm}^{-1}$ . Compare this to typical RAIR spectra in the literature that are recorded at  $4\text{ cm}^{-1}$  resolution. That basically means a mirror travel increase from 0.25 cm to 10 cm and hence an increase in measurement time at fixed mirror velocity of at least 40 times. Typically at  $4\text{ cm}^{-1}$ , a basic spectral scan of 256 co-added interferograms would take a few minutes. At  $0.1\text{ cm}^{-1}$ , this increases to over an hour. However, the S/N of the resulting data is reduced by enhanced noise contributions from the source, spectrometer and surroundings. We could recover this by increasing the number of co-added interferograms but this only scale by the standard factor of  $\sqrt{N}$  (the total number of co-added scans) which would mean at a 4 fold increase in time to get even a 2 fold increase in S/N taking the scan time from over an hour to over 4 hours! This is not practical and we made the logical decision to work as described in the experimental section.

An addition in **bold** has been made to the text as follow:

“The TPD data for CO desorbing from aSiO<sub>2</sub> are shown in Figure 2 and exhibit coincident trailing edges at low exposures and a common leading edge at higher exposures **as shown in the insert. The dashed lines are the results of sub-monolayer  $E_{\text{des}}$  simulations based on a previously used FORTRAN 90 model<sup>24</sup>, the use and relevance of this model will be discussed later in this section.** The data in the insert is consistent with multilayer growth as seen from the clear shift in the leading edge of desorption. This allows us to...”

And the figure has been changed to the one as also seen below:





This figure also includes details as to why we have chosen to use the average desorption energy curve for the IR model. The present figure as shown above also shows the results of desorption simulations in dashed lines (details of the simulation can be found in reference 24 of the manuscript). The average desorption energy was used to create this model and correlates both with the data and the idea that desorption peaks should shift to lower temperature/lower  $E_{\text{des}}$  as the coverage increases.

The following has been added to the text to highlight the addition of the  $E_{\text{des}}$  simulation:

“A full analysis involving models of the experimental CO data have previously been detailed for the substrate used in this work<sup>19</sup> and other aSiO<sub>2</sub> surfaces.<sup>27</sup> **The averaged data as seen in the insert in Figure 3 will be used from hereon as a representation of the distribution of interaction energies of CO molecules with the aSiO<sub>2</sub> surface. Our basis for saying this can be seen when returning to Figure 2. Here, the dashed lines are the results of sub-monolayer desorption simulations where the coverage dependant  $E_{\text{des}}$  from the insert in Figure 3 is used in the simulation of all our TPD measurements. As can be seen in Figure 2, the data and simulations are consistent and shift toward lower temperature as the coverage increases. This is as expected, when wetting molecules transition from sub-monolayer, to monolayer and on to multilayers. With this said, we use the averaged  $E_{\text{des}}$  distribution from Figure 3 to derive the likelihood of CO adsorption at a particular site with a given  $E_{\text{des}}$  *i.e.*, the value of  $P(E_{\text{des}})$ .  $P(E_{\text{des}})$  is given by (5):**

$$P(E_{\text{des}}) = -\frac{dN_{\text{ads}}}{dE_{\text{des}}} \quad (5)$$

Figure 4 shows  $P(E_{\text{des}})$  versus  $E_{\text{des}}$  for the CO-aSiO<sub>2</sub> system under consideration. The distribution recovered is not dissimilar to those...”

Can the authors repeat the experiment(s) plotted in Fig. 1 (and perhaps Fig. 6) to be able to extract an average FWHM as well as an estimate of the reproducibility of the 0.6 ML curve in

Fig. 3? Similar for an experiment with 1.0 ML to ensure the quantification of a single monolayer.

To comment on this question we have created a new table with data from the TPD and RAIRS experiments. The table and following text is now in the manuscript:

CO Coverage / ML	$E_{\text{des}} / \text{kJ mol}^{-1}$ ( $\pm 0.5$ )	FWHM / $\text{cm}^{-1}$ ( $\pm 0.1$ )	$\delta / \text{cm}^{-1}$ ( $\pm 0.05$ )
0.2	8.1 – 9.6	5.0	2.1
0.4	7.6 – 10.2	5.4	2.3
0.6	7.3 – 8.9	5.6	2.5
0.8	6.9 – 9.0	6.5	2.8
1.0	6.2 – 9.0	6.7	2.9

Table 1: This table shows the experimental values extracted from the TPD and RAIRS experiments of the various CO coverages.  $\delta$  are the linewidths of the  $\nu\text{CO}$  features.

Along with the table, the following text has been added to the manuscript as a new paragraph:

“... Hence,  $S$  is 1.

**A summary of the experimental results can be seen in Table 1. The range of  $E_{\text{des}}$  values decrease with increasing coverage as expected and illustrated in the literature.<sup>19,27</sup> The uncertainty related to the desorption energy stems from the uncertainty in the temperature measurements ( $\pm 0.5$  K). FWHM measurements of each coverage are shown as estimated from the baselined RAIR spectra where the uncertainty is due to the resolution of the FT-IR spectrometer ( $\pm 0.1 \text{ cm}^{-1}$ ). The linewidth is calculated from the FWHM as stated in Equation 8, however this will be discussed in further detail later in this work.”**

Please state if one monolayer corresponds to  $1\text{e}15 \text{ cm}^{-2}$ .

The rate at which molecules interact with the surface can be calculated through this equation:

$$N_{\text{total}} = Z_{\text{wall}} t = \frac{PSt}{\sqrt{2\pi m k_B T}}$$

This is a reasonable approach considering the low pressure, lack of contaminants in the UHV chamber and with an assumed sticking coefficient of unity. Considering this, and while checking the CO purity, we say that any increasing the pressure when the leak valve is opened, is purely due to CO.

By conducting TPD experiments with different film thicknesses there changes in the TPD profiles and shifts in the leading edges. At some stage, the monolayer to multilayer regime will be encountered. In the case of this work, this happened between 8 L to 10 L.

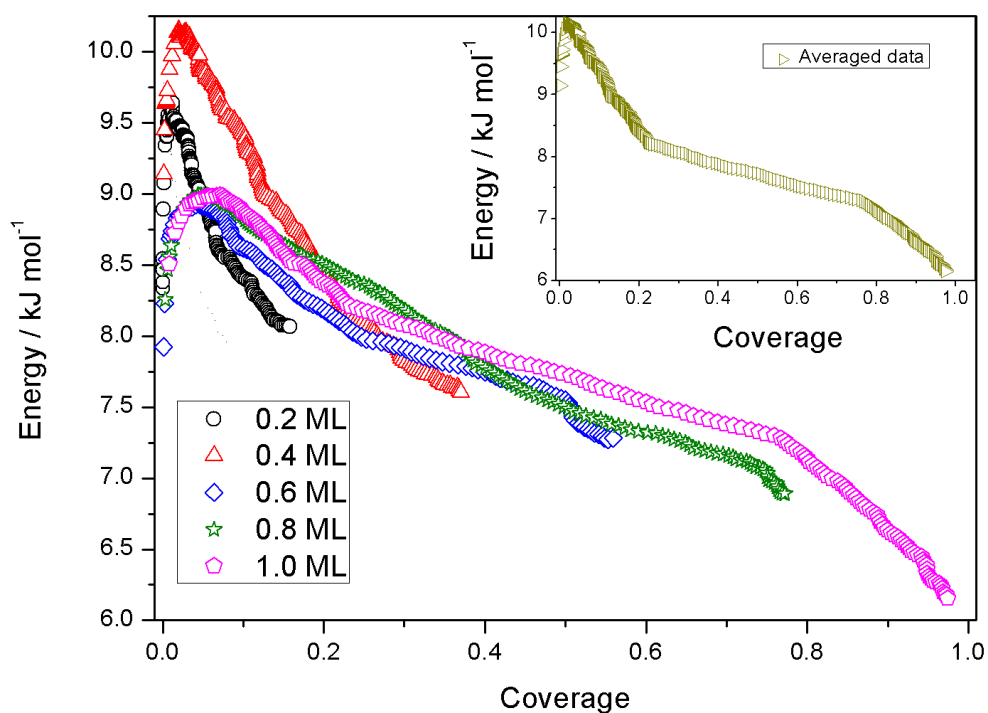
Backtracking from this stage and considering 10 L as being 1 ML, we use the pressure for 1 second equivalent to 10 L to calculate the number of molecules in 10 L as being  $2.88 \times 10^{15}$  molecules  $\text{cm}^{-2}$  which is our estimate of 1 ML.

We have added the following **bold** addition to the text to let the reader know what our estimate ML is in terms of molecules:

“The latter is consistent with multilayer growth and allows us to identify the exposure necessary to generate a monolayer coverage on the aSiO<sub>2</sub> surface **which is estimated to contain  $2.88 \times 10^{15}$  molecules  $\text{cm}^{-2}$ .**”

It is said that 'Plots of  $E_{\text{des}}$  against  $N_{\text{ads}}$  are constructed'. Can the authors explain the procedure, e.g., how is the separation of the data points in Fig. 3 determined? The TPD spectra are recorded continuously, so I assume that there is a choice made in terms of binning datapoints?

The overall exponential fits were conducted with all data points. The data in Figure 3 contains “skipped data points” meant to make the figure easier to read and less crowded. The actual amount of data points are shown below (and now also in the manuscript):



The procedure for developing the TPD data, *i.e.* from the experimental data in Figure 2 to Figure 3 has been added to the text:

“Plots of  $E_{\text{des}}$  against  $N_{\text{ads}}(t)$  are constructed for each sub-monolayer CO dose (Figure 3) **from the experimental data presented in Figure 2 along with Equations 2, 3 and 4.** A full analysis involving models of the experimental CO data have previously been detailed for the substrate used in this work<sup>19</sup> and other aSiO<sub>2</sub> surfaces<sup>27</sup>.”

The authors refer repeatedly to the work of Noble et al. MNRAS 454 2636 2015; in this study  $p(E)$  is assumed to be given by Fermi-Dirac statistics. Can the authors comment on the relation or similarities of their observed  $P(E)$  plotted in Fig. 4 to expression (7) of Noble et al.?

The Noble *et al.* binding sites are described by a binding energy distribution which is a symmetric Gaussian function. From here they use the Fermi-Dirac statistical equilibrium to find the probability. Then they go on to integrate  $P(E_{\text{des}})dE$  to find  $N$ . This last step is the same step we use for the sub-monolayer TPD analysis.

In effect from Nobel *et al.*'s 8<sup>th</sup> equation, it seems they use the  $P(E_{\text{des}})$  to find  $N$  through  $E_{\text{des}}$  whereas analysis in this work relies on the same theory, but reversed. We have used  $N$  and  $E_{\text{des}}$  to find  $P(E_{\text{des}})$ . So, there is a common basis in the two papers, but used for different purposes.

Is the average curve in the inset of Fig. 3 used to create Fig. 4?

The average curve in the inset in Fig. 3 is indeed used to create Fig. 4. By creating this average data curve we sample all CO coverages and their interactions with the surface. This makes for a simple way to compare such interactions with the experimental IR data.

On page 3, point 2, please rephrase the explanation on the vibrational origin  $\nu_0$ .

We understand the possible issue readers may have when we mention vibrational origin in this respect. Vibrational origin in vibrational spectroscopy is the position of a rotation free vibrational frequency in the rovibrational spectrum and we do not have any CO rotation in the experiments. So, we have removed mention of this and left the text as:

"where  $\bar{\nu}_0$  can be thought of as representing the vibrational wavenumber of CO on non-interacting aSiO<sub>2</sub> surface, *i.e.* it encompasses the effect of the mass of the silica surface on the CO vibration"

Please expand on the text currently in the caption of Fig. 5 and move it to the main text: *e.g.*, why are different linewidths (0.1 and 2.5 cm<sup>-1</sup>) used and why is the best-fit linewidth of Fig. 5B not equal to that in Table 1?

The new figure caption now reads as follows:

**"Figure 5:** Comparison of the experimental (open circles) and modelled (red line) data of CO on aSiO<sub>2</sub>. The experimental data is of 0.6 ML CO at 18 K and exhibits a FWHM of 5.6 cm<sup>-1</sup>. **(A)** shows the simulated line profile when CO is ballistically deposited with a FWHM of 12.5 cm<sup>-1</sup>. **(B)** shows how a better fit is obtained when CO is free to diffuse using the inverse Boltzmann weighted distribution of  $E_{\text{des}}$  and leads to a best-fit FWHM of 5.9 cm<sup>-1</sup>. A point to note is the sub-structure in the experimental line profiles which is due to overlapping features from gas-phase water in the optics purge gas outside of the UHV chamber."

The general text has been changed to include the information removed from the caption. The additions have been marked with **bold**:

“This would represent the situation where the CO is ballistically deposited, *i.e.* random deposition without subsequent diffusion on the surface (“stick and stop” as it is sometimes referred to). **The model shown in Figure 5A is the best fit given the ballistic deposition conditions and does not fit the data well. The model is made from the full  $E_{\text{des}}$  distribution from Figure 4 and a simulated linewidth of  $2.5 \text{ cm}^{-1}$  (compared to the experimental resolution of  $0.1 \text{ cm}^{-1}$ ) which yields a FWHM of  $12.5 \text{ cm}^{-1}$ .** On the other hand, Figure 5B illustrates the effect of restricting”

The text already contains all the information regarding Figure 5B.

In order to clarify the statements made about the dangling OH bond and its importance, have the authors considered to perform an experiment on compact amorphous water or on CH<sub>3</sub>OH (concerning the latter; please see also the discussion about the  $2152 \text{ cm}^{-1}$  band in Cuppen *et al.* MNRAS 2011 417 2809)?

This is an interesting question indeed. Changing the number of dangling OH dangling bonds will change the relaxation route into a possible phonon bath. Porous ASW (as used in the presented experiments) presents a large number of OH dangling bonds. This number decreases as ASW becomes compact ASW. Experiments with compact and crystalline water will be conducted in the near future. In contrast, CH<sub>3</sub>OH is known not to present dangling OH bonds at its surface. Comparison of the other forms of water ice and of CH<sub>3</sub>OH ice would be very interesting and is something we are currently investigating.

The work of Cuppen *et al.* looking at the non-detection of the  $2152 \text{ cm}^{-1}$  feature from ISM spectra is very interesting. The feature at  $2152 \text{ cm}^{-1}$  has been regarded for a long time and they do great experiments with H<sub>2</sub>O/CO/CO<sub>2</sub> mixtures showing this feature and CO/CH<sub>3</sub>OH mixtures showing the lack of feature. All of the Cuppen *et al.* experiments are of mixtures, while we have kept the experiments layered to test the concept of relating IR and TPD data.

The final paragraph on Page 4 may be rephrased for reasons of clarity.

This paragraph has been changed and now reads as this:

“Figure 6 shows the ballistic deposition and diffusive models as compared to the experimental data. This could indicate that CO is free to both hit-and-stick and diffuse at the same time. Comparing  $E_{\text{des}}$  values for CO on aSiO<sub>2</sub> ( $6 - 12 \text{ kJ mol}^{-1}$ ) and CO on p-ASW ( $11 - 16 \text{ kJ mol}^{-1}$ )<sup>29</sup> indicates that CO is more strongly bound to the water surface. A widely accepted rule of thumb says that the barrier to surface diffusion is of the order of  $10 - 15\%$  of the system’s  $E_{\text{des}}$ <sup>32</sup>. This leads to CO being freer to diffuse on aSiO<sub>2</sub> as compared to p-ASW, which can also be understood from Figure 5 and 6. Recent work<sup>33-35</sup> suggests that CO is relatively free to diffuse while about  $10\%$  CO molecules on p-ASW can be trapped in pores. This is also seen in Figure 6 as both a ballistic deposition model and a diffusive model fit the experimental data. From the experiments and data presented in this work, an amount of CO trapped or mobile cannot be estimated. However, while developing our

thoughts from references [33 – 35] we suggest a diffusive model represents the experimental data to a better degree considering the FWHM as shown in Table 2.”

### Conclusion

It is said that the approach described here is 'generalizable'. Do the authors have data available on other small molecules or is this available in literature? It could well be that CO is much more sensitive to its surroundings as a result of the electronic structure and its ability to interact with a dangling OH. I would not expect a molecule like CH<sub>4</sub> for instance to allow similar observations and therefore I wonder about the possibility to generalize the study.

We plan on furthering the idea of synthesising sub-monolayer molecular data from TPD to IR by looking at other non-wetting molecules. What we mean about generalizable is that sub-monolayer coverages of wetting molecules will interact with the surface. This interaction is probed through TPD and IR experiments which can hopefully be related through the ideas proposed in this manuscript. We do not currently have any additional data on other molecules to report, however CH<sub>4</sub> is an interesting example as it behaves similarly to CO on ASW surfaces.

Page 3 - Typo:

"Given then we are considering ..." --> "Given that we are considering..."

This has been changed, thank you for spotting the typo.

Referee: 2

Comments to the Author

This is a very nice paper. It is clearly written, well argued and the conclusions are all sound and backed up with relevant evidence. The authors show a method for determining a range of binding energies for a species on a surface. They illustrate how this works for their own data. Importantly, they then show how this can also be used for other data (that of Kay et al), showing that the method and the conclusions they use have broad applicability. The paper is very clear and in my opinion is suitable for publication without any changes being needed.

We thank the reviewer for the time spent in reading our work and commenting on our work.